Flow Pattern Visualization of Combined Sewer Overflow

Vojtěch Bareš, Jaroslav Pollert, Petr Srníček
Department of Sanitary and Ecological Engineering, CTU Prague, Thákurova 7, 166 29, Prague 6, Czech Republic, email: bares@fsv.cvut.cz; pollertj@fsv.cvut.cz; petr.srnicek@fsv.cvut.cz

Presented paper deals with 2D flow visualization using Ultrasonic Doppler Method (UDM). The flow patterns in the axes of plane symmetry of designed combined sewer overflow (CSO) were measured on the hydraulic model made of plexiglass using Ultrasonic Velocity Profile (UVP) Monitor. The experiments were focused on both, the optimalization of CSO geometry and the verification of the 3D CFD model. The results show great potential of the UDM in combination with numerical analysis to visualize 2D flow field. Moreover, the optimal geometrical configuration with respect to the gravitational separation of suspended solids content and separation of floatable solids was found as well. The comparison between experimental values and CFD simulations introduces sufficient agreement.

Keywords: CFD, flow visualization, receiving water, sewer, ultrasonic Doppler method, velocity profile

1 INTRODUCTION

Combine sewer overflow (CSO) represents a crucial sewer structure related to wet-weather pollution in urban areas. A tremendous number of CSOs geometrical configurations were developed during last decades worldwide. Often, the geometry of CSO is given by regional development routine and varies in the wide range even in the particular countries. The CSO design itself should take into account different criteria as hydraulic behavior, discharge distribution, energy losses, separation of floating solids, cost-effectiveness etc. In addition, the efficiency of the separation of suspended solids content should be increased using the optimal hydraulic condition and flow pattern distribution. Therefore, the authors deal in the presented study with an evaluation of new prefabricated CSO unit made of fiberglass tubes based on the methods of hydraulic and numerical simulations.

Today, Particle Image Velocimetry (PIV) is most often used method for instantaneous flow pattern visualization. However, various measuring techniques are applicable as well. Mavros (2001) discussed application of wide spectra of methods (hot-wire anemometry, laser Doppler anemometry, laser-induced fluorescence or PIV) with the respect to their usefulness for particular situations. The usability of ultrasonic Doppler method (UDM) for flow visualization was demonstrated e.g. by Murai et al. (2004) at vortex ring dynamics or Hersberger (2003) at curved channel flows, who in fact mainly determined 2D or 3D time-averaged velocity vectors only, when distinctively more simple measuring configuration can be used.

Therefore, the paper deals with simple technique of 2D time-averaged flow field visualization using UDM, particularly UVP method [4]. The flow patterns in the axes of plane symmetry of designed CSO were measured on the hydraulic model made of plexiglass under laboratory condition. The technique is based on measurements with one ultrasonic probe only, its variable spatial positioning and affine matrix transformation. The obtained velocity vector maps were used for both, the optimalization of CSO geometry and the verification of the 3D mathematical model.

2 CSO DESIGN AND OPERATING PRINCIPLES

Due to both manufacturing and construction expenses a very simple principle for CSO design was applied.

In fact, CSO consists of two pipes positioned one above the other (Fig. 1). The outlet with flow regulator is connected at the end of the lower inlet pipe. The upper pipe with slit gate at the bottom along the whole connection of both pipes serves as wastewater overflow into receiving waters. Upstream the slit gate, downflow baffle was installed to prevent the wash-out of floatable solids to natural water environment. Three basic shapes (width) of the slit gate were tested (hereafter lettered as ST1-ST3).

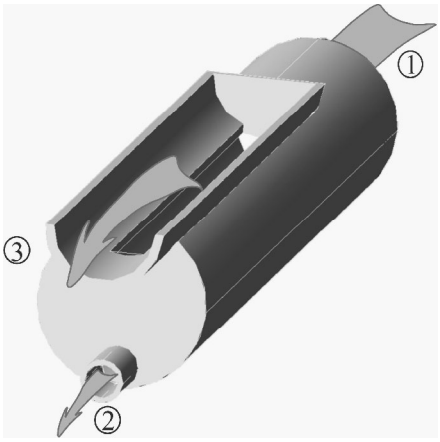

Figure 1: Axonometric projection of CSO chamber (1. inlet; 2. outlet to waste water treatment plant (WWTP); 3. overflow cross slit gate to receiving waters).

2 METHODS

2.1 Experimental setup

Experimental apparatus (Fig.2) was assembled by hydraulic model of CSO itself, electronically controlled valve, mixed tank with pump for injection of tracking particles and devices for measurement of hydraulic quantities.

Particularly, two MID flowmeters were installed at the inlet and outlet of CSO. Free-surface longitudinal profile was measured using water level point gauge and US water level transducers.

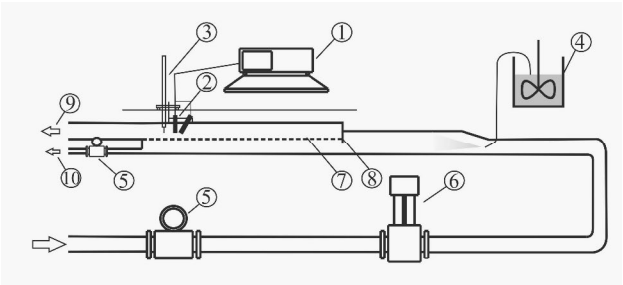

Figure 2: Experimental setup (1. UVP unit; 2. US transducers; 3. movable point gauge and US water level probe; 4. mixing tank; 5. flowmeters; 6. valve; 7. overflow crest; 8. downflow baffle; 9. CSO overflow; 10. CSO outlet towards WWTP).

2.2 Velocity measurements

The instantaneous information about velocity distribution in mid-vertical plane of symmetry of CSO was obtained using UVP Monitor (Met-Flow, S.A.). By reason that only time-averaged value of the velocity vectors were analyzed, one US transducer in 3 different geometrical position was used (hereafter: lettered as $S_{1,2,3}$). S_1 was mounted vertically within Cartesian coordinates $[x_K,y_K]$ and others ($S_{2,3}$) under angle $\beta = \pm 25°$ from vertical axis (Fig. 3). Moving longitudinal drive along horizontal axis in 50 mm step 24×3 radial velocity profiles $V_{1,2,3}(y_K)$ were measured .

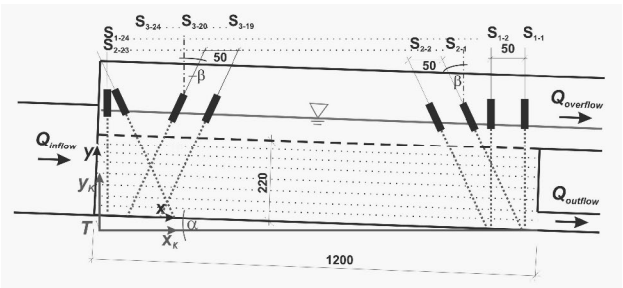

Figure 3: Detail of probe positioning.

2.3 CFD simulation

CFD simulations of 3D flow field of CSO were executed in FLUENT environment. Free surface was simulated as a wall without friction. Experimentally evaluated longitudinal profile of free surface along the overflow pipe was considered as boundary condition. Tetrahedral mesh with different density was used due to increasing precision in overflow silt gate. Further, one geometrical configuration of CSO of the model was simulated using various types of turbulence models to choose optimal one (standard k-ω model). As a criteria, RMS of horizontal and vertical velocity components related to UVP measurements at mid-vertical plane of CSO symmetry over whole measured flow field were chosen.

3 DATA ANALYSIS

3.1 Velocity vectors decomposition

Velocity vectors decomposition takes into account several specific aspects of experimental setup as follows: *i)* coordinates of discrete measuring elements given by each US probes $S_{1,2,3}$ are unequal; *ii)* velocity vectors in discrete measuring elements are measured in direction of radial axis of US probes $S_{1,2,3}$; *iii)* coordinate system of CSO model $[x,y]$ is different from Cartesian coordinate system $[x_K,y_K]$.

Considering above mentioned aspects leads to necessity to transform coordinates of discrete measuring elements from Cartesian $[x_K,y_K]$ to CSO $[x,y]$ coordinate system (Figure 3). In case of probe S_1 one can write:

$$[x_1, y_1] = \Re \cdot [x_{K1}, y_{K1}] + T \tag{1}$$

$$\Re = \begin{vmatrix} \cos a & -\sin a \\ \sin a & \cos a \end{vmatrix} \tag{2}$$

where $\Re$ is rotation by angle α and T is shift vector of the origin (Fig. 3).

Whereas the US probe S_2 is rotated from the vertical by angle β eq. (1) is expressed as:

$$[x_2, y_2] = D \cdot \Re \cdot [x_{K2}, y_{K2}] + T \tag{3}$$

where D is a diagonal matrix expressing skewing of measured matrix $[x_{K2},y_{k2}]$ by angle $\beta = 25°$ (Fig. 3) given as:

$$D = \begin{vmatrix} 1 & \sin b \\ 0 & 1/\cos b \end{vmatrix} \tag{4}$$

Similarly, one can write eq. (3-4) for probe S_3 with D related to negative value $\beta = -25°$ (Fig.3).

Consequently, 2D bilinear interpolation [5] of radial velocity vectors $V_{1,2,3}$ from matrices $[x_{1,2,3},y_{1,2,3}]$ to arbitrarily defined rectangular grid is required (herein: measured element size 1220×220 mm; grid spacing 10×10 mm; nr. of grid points 2783).

Finally, one can define total velocity vector and its components in all nodes of the grid. At least couple of measured radial vectors (either $[V_1,V_2]$ or $[V_1,V_3]$) is known in each grid point. Therefore, following expressions for $[V_1,V_2]$ can be defined:

$$V_1 = v_{YK} \tag{5}$$

$$V_2 = v_{YK}\cos b - u_{XK}\sin b \quad (6)$$

For total vector *U* one can simply write:

$$U = \sqrt{u_{XK}{}^2 + v_{XK}{}^2} \quad (7)$$

Accordingly, replacing $V_2 \rightarrow V_3$ in eq. (6) provides solution for $[V_1, V_3]$.

3.2 Numerical model data transformation

The 3D grid of modern computational tools is created by irregular elements which created 2D triangular mesh with variable density in mid-vertical plane of CSO symmetry. Therefore, resampling of the hybrid triangular mesh $[x_f, y_f]$ to defined rectangular mesh $[x_s, y_s]$ is required to proper calibration and verification of CFD model using experimental data sets.

In fact, the transformation can be described by 2D interpolation of vector components *u, v* in random distributed nodes $[x_f, y_f]$ to defined rectangular mesh $[x_s, y_s]$ using both the Delauny triangulation [5] and the triangular interpolation itself [6].

4 RESULTS

4.1 Evaluation of CSO geometry using UVP

Different geometrical configurations of CSO were evaluated with respect to minimized vertical velocity components (minimizing sewer solids wash-out). Flow patterns of measured element of CSO were analyzed using above described methodology. Fig. 4 presents velocity colour map with total vector field.

Developing sweep region (x = 200 ÷ 400 mm) can be clearly seen (Fig. 4, Fig. 5) for silt gate shapes *ST1* and *ST2.* Horizontal velocity profiles of vertical velocity *v(x)* (Fig. 5) well demonstrate this effect. The difference between maximal vertical velocity components for all at the end of the silt gate (x = 1200 mm, y = 210 mm) is however negligible.

Moreover, in accordance with previous assumptions the formation of eddy structure can be observed at x = 300 ÷ 500 mm for *ST1* (Fig. 4, Fig. 6).

On the other side, the change of slit gate geometry influences significantly the size of the dead zone downstream of the downflow baffle. Fig. 4 and Fig. 6 demonstrate developing of dead zone. Velocity profiles *u(y)* are almost identical at x = 700 mm, but upstream profiles are strongly affected. *ST3* shows the worst results (almost 40 % of the slit gate is useless).

4.2 Calibration of CFD model

Beside that, obtained data sets were used for numerical model calibration and verification. However, preliminary experiments shows only week possibilities to optimize model parameters e.g. wall friction etc. due to low sensitivity of tested parameters.

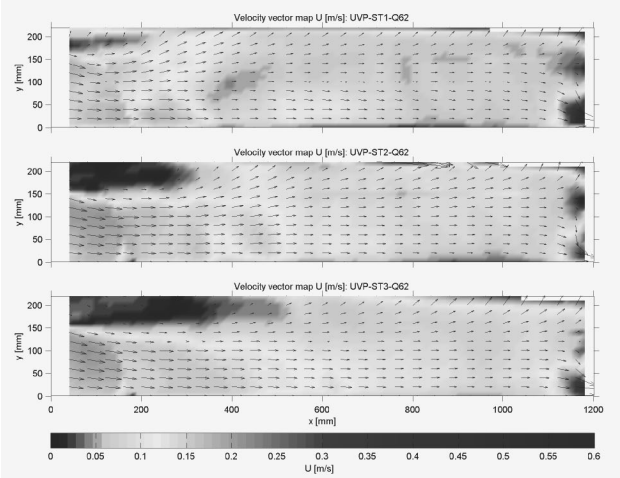

Figure 4: Flow pattern visualization with total vector map of CSO element for different geometrical configurations of slit gate (*ST1, ST2* and *ST3*).

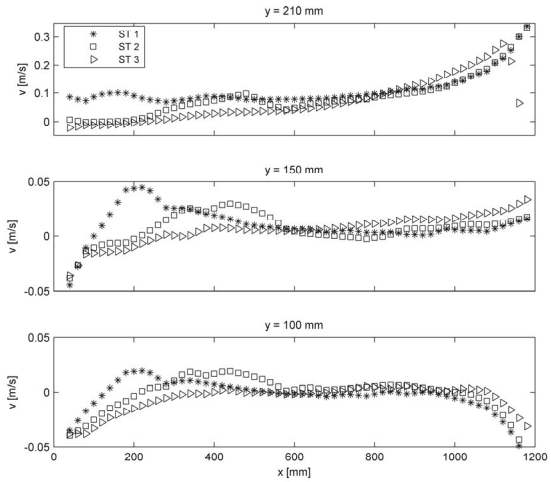

Figure 5: Horizontal profiles of vertical velocity components *v(x)* for coordinates y = 100 ÷ 210 mm and different geometrical configuration.

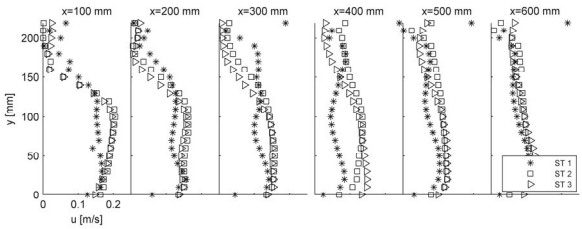

Figure 6: Developing of vertical profiles of longitudinal velocity components *u(y)* for coordinates x = 100 ÷ 1100 mm and different geometrical configuration.

Therefore, attention was called to compare different turbulence models supported by FLUENT (standard k-ε, RNG k-ε, realizable k-ε, standard k-ω, shear stress transport (sst) k-ω, Spallart-Allmaras (SA)) with respect to best results. Generally, all simulations provide comparable results to UVP measurements. However, one can find significant deviations in specific regions. Particularly, in the

dead zone downstream the downflow buffle standard k-ε, realizable k-ε and *SA* significantly overvalue real horizontal components *u* (Fig. 7). It can be also demonstrated on vertical components *v* (Fig. 8). On the other side, second group of models overestimates results in a bulk flow (Fig. 7). Further, all models significantly overestimate vertical components of velocity *v* (Fig. 8).

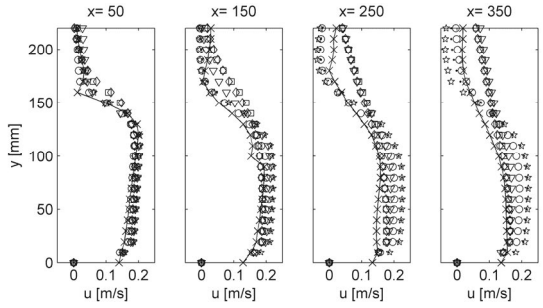

Figure 7: Vertical profiles of horizontal velocity component *u(y)* for UVP (-x-) and CFD simulations (▽ - SA; ♢ - standard k-ε; ☆ - RNG k-ε; □ - realizable k-ε; ○ - standard k-ω; • - sst k-ω).

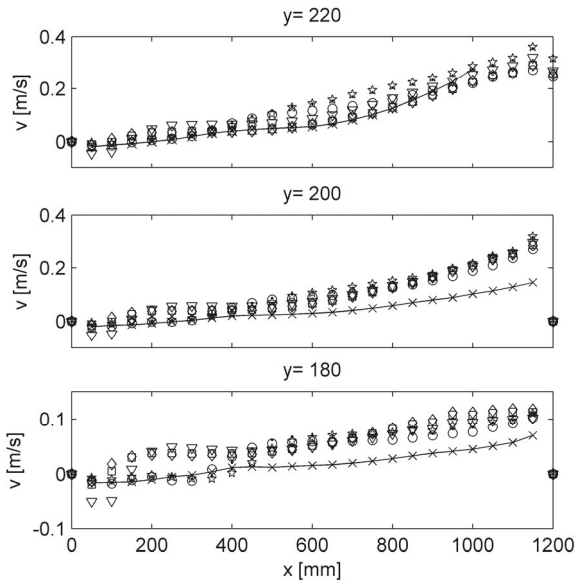

Figure 8: Horizontal profiles of vertical velocity component *v(x)* for UVP (-x-) and CFD simulations (▽ - SA; ♢ - standard k-ε; ☆ - RNG k-ε; □ - realizable k-ε; ○ - standard k-ω; • - sst k-ω).

Calculating RMS of horizontal and vertical components deviation between CFD simulation and hydraulic modeling (Fig. 9) best fitted turbulence model was chosen (standard k-ω) for further optimalization of CSO geometry.

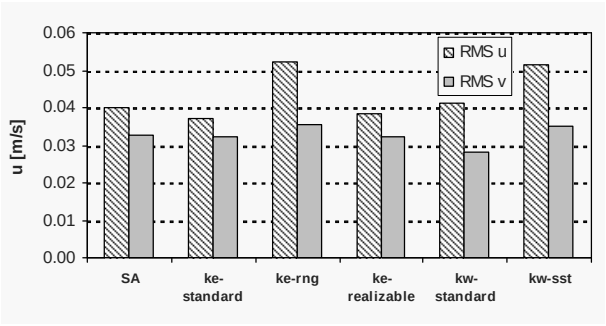

Figure 9: RMS of *u* and *v* for applied turbulence models.

6 SUMMARY

The optimal geometrical configuration of proposed CSO with respect to the gravitational separation of suspended solids content and separation of floatable solids was found using combination of hydraulic and CFD simulations.

The results show great potential of simple application of the ultrasonic Doppler method in combination with numerical data analysis and affine matrix transformation to visualize 2D flow field. However, presented methodology allows obtaining the time-averaged velocity flow field only.

The comparison of experimental data with CFD turbulence models shows wide range of possible simulation results. It's obvious, that "blind" CFD application without careful validation can lead to results misinterpretation.

ACKNOWLEDGEMENT

This work was supported by the Czech Science Foundation; project No.103/04/1350, by the project of Czech Ministry of Education, Youth and Sport No. MSM6840770002 and by HOBAS CZ, Ltd.

REFERENCES

[1] Mavros P: Flow visualization in stirred vessels - A review of experimental techniques, Chemical Engineering Research and Design, 79 (A2) (2001) 113-127.
[2] Murai Y, Kitaura H, Xiao Z, Thomas PJ, Takeda Y: Study of Vortex Ring Dynamics using UVP, Proceedings 4th ISUD, Sapporo, (2004) 3-8.
[3] Hersberger DS: Wall roughness effects on flow and scouring in curved channels with gravel bed, PhD thesis, EPFL Lausanne (2003).
[4] Takeda Y: Instantaneous Velocity Profile Measurement by Ultrasonic Doppler Method, JSME International Journal (1995) 8-16.
[5] Sedgewick R: Algorithms in C, Part 5: Graph Algorithms, Addison-Wesley, Reading (2002).
[6] Press WH, Flannery BP, Teukolsky SA, Vetterling WT: Numerical Recipes in C. The Art of Scientific Computing, Cambridge University Press (1993).